20th Australasian Fluid Mechanics Conference
Perth, Australia
5-8 December 2016

Characteristics of energy dissipation in a turbulent cylinder wake

J.G. Chen[1], Y. Zhou[1], R.A. Antonia[2], T.M. Zhou[3]

[1]Institute for Turbulence-Noise-Vibration Interactions and Control,

Shenzhen Graduate School, Harbin Institute of Technology, Shenzhen 518055, China

[2]School of Engineering, University of Newcastle, NSW 2308, Australia

[3] School of Civil, Environmental and Mining Engineering, The University of Western Australia,

35 Stirling Highway, Crawley, WA 6009, Australia

Abstract

This work aims to improve our understanding of the turbulent energy dissipation rate in the turbulent wake of a circular cylinder. Ten of the twelve components are simultaneously measured at nominally the same point across the wake with a vorticity probe which comprises 4 x-wires. A phase-averaged technique is applied to the energy dissipation rate estimation to examine the spatial topology of both the coherent (large-scale) and remaining (small-scale) components of the turbulent energy dissipation rate. It is found that the distribution of the energy dissipation occurs mostly within the spanwise vortex rollers, rather than in regions where turbulent mixing is important. This new information has been incorporated into Hussain and Hayakawa's [6] flow structure model in order to reflect the topological characteristics of the energy dissipation rate in the near/intermediate region of a plane wake.

Introduction

The mean turbulent kinetic dissipation rate, which plays a major role in small-scale turbulence research [10] is given by

$$\begin{aligned}\overline{\varepsilon} &= \nu\overline{u_{i,j}(u_{i,j}+u_{j,i})} \\ &= \nu\Big\{\underbrace{2\overline{u_{1,1}^2}}_{1}+\underbrace{\overline{u_{2,1}^2}}_{2}+\underbrace{\overline{u_{3,1}^2}}_{3}+\underbrace{\overline{u_{1,2}^2}}_{4}+\underbrace{2\overline{u_{2,2}^2}}_{5}+\underbrace{\overline{u_{3,2}^2}}_{6} \\ &\quad+\underbrace{\overline{u_{1,3}^2}}_{7}+\underbrace{\overline{u_{2,3}^2}}_{8}+\underbrace{2\overline{u_{3,3}^2}}_{9}+\underbrace{2\overline{u_{1,2}u_{2,1}}}_{10}+\underbrace{2\overline{u_{1,3}u_{3,1}}}_{11}+\underbrace{2\overline{u_{2,3}u_{3,2}}}_{12}\Big\}\end{aligned} \quad (1)$$

where an overbar indicates a time-averaged quantity; ν is the kinematic viscosity; $u_{i,j} \equiv \partial u_i/\partial x_j$ is the derivative of velocity fluctuation u_i in x_j direction; i and j = 1, 2, and 3 representing the streamwise, lateral and spanwise directions, respectively, are used interchangeably with x, y and z (see figure 1). Significant attention has been paid to the behaviour of $\overline{\varepsilon}$ in various flows, either by experiments or numerical simulations. Browne *et al.* [2] measured the nine major terms (1-9 in equation (1)) of $\overline{\varepsilon}$ in a turbulent far wake (x/d =420, where d is the diameter of the cylinder), and found that $\overline{\varepsilon}$ based on the isotropy assumption may underestimate the total dissipation rate by 45%~80% across the wake. Both [4] and [9] suggest that $\overline{\varepsilon}$ estimated using the assumption of local axisymmetry is closer to the true value than that estimated based on the assumption of local isotropy in most turbulent shear flows. More recently, using DNS data, Lefeuvre *et al.* [8] found that in the turbulent intermediate wake (x/d = 10-100) of a square cylinder, the approximation of $\overline{\varepsilon}$ based on the assumption of local homogeneity in the transverse plane, i.e. (y, z) plane, can provide the most accurate surrogate of the energy dissipation rate. A similar result may be expected in the wake of a circular cylinder which generates a less isotropic wake than a square cylinder [12]. One can expect that the isotropic approximation of $\overline{\varepsilon}$ will approach the true value of $\overline{\varepsilon}$ as the Reynolds number increases, as has been confirmed by Tang *et al.* [11].

Hussain and Hayakawa [6] proposed a topological model for the mechanism of a turbulent plane wake, where the turbulence production occurs mainly along the diverging separatrix and the turbulent mixing takes place in the region where the ribs and rollers are in contact with each other. However, information on the spatial distribution of the turbulent energy dissipation is not provided in the model. Landau and Lifshitz [7] commented that the energy dissipation rate had to be considered as a fluctuating quantity, in the same manner as any other fluctuating quantity which is likely to be affected by the large scale motions. Therefore, it is of great importance and interest to investigate how the spatial organization of the turbulent energy dissipation is affected by the Kármán vortices.

The present investigation focuses mainly on the characteristics of the energy dissipation rate in a turbulent cylinder intermediate wake (x/d = 10 - 40), the special attention being paid to its spatial distribution in the context of the strong coherent Kármán vortex street. In the present study, except for the 5th and 9th terms in equation (1), ten out of the twelve terms are simultaneously captured with a probe consisting of four x-wires. After selecting the best approximation for $\overline{\varepsilon}$, a phase-averaging technique is used to examine the spatial organization of $\overline{\varepsilon}$, with respect to both large and small scales.

Experimental Details

Experiments were conducted in an open-loop low turbulence wind tunnel with a 2.4m-long working section(0.35m × 0.35m). A circular cylinder with a diameter d = 12.7mm was used to generate the wake. The free-stream velocity U_∞ = 3.0 m/s. The Reynolds number Re ($\equiv U_\infty d/\nu$) is 2.5×10^3. A movable probe (figure 1(b) & (c)) consisting of four x-wires was used to measure the velocity fluctuations and their derivatives simultaneously at nominally the same point in the flow. The separation between the two inclined wires of each cross-wire was about 0.6mm. Two of the X wires, b and d, were aligned in the (x, y) plane and separated by Δz = 1.9mm; the other two, a and c, were separated in the (x, z) plane by Δy = 1.9mm. Measurements were made at x/d =10, 20 and 40. The output signal from the anemometers was passed through buck and gain circuits and low-pass filtered at a cut-off frequency f_c close to the Kolmogorov frequency $f_k = \overline{U}_1/2\pi\eta$, where $\overline{U}_1$ is the mean streamwise velocity on the centerline of the wake and $\eta \equiv (\nu^2/\overline{\varepsilon})^{1/4}$ is the Kolmogorov length scale. The filtered signal was subsequently sampled at a frequency $f_s = 2f_c$ (3200Hz at x/d=10 and 20; 2500Hz at x/d=40) using a 12-bit A/D converter. The record duration was about 60s.

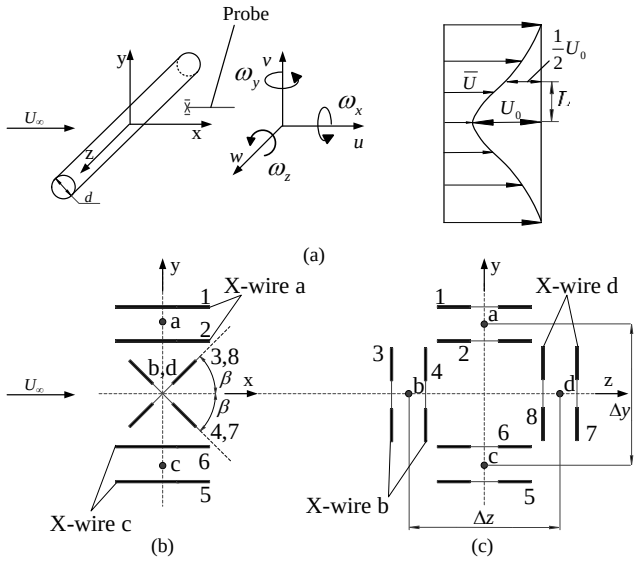

Figure 1. (a) Experimental arrangement, coordinate system, and definition sketch; (b) side view of the vorticity probe; (c) front view of the probe.

x/d	U_0/U_∞	L/d	$\overline{\varepsilon}$ (m^2/s^3)	η (mm)	$\Delta x/\eta$	$\Delta y/\eta$	$\Delta z/\eta$
10	0.22	0.64	4.03	0.17	4.8	11.2	11.2
20	0.18	0.88	1.63	0.21	3.9	9.0	9.0
40	0.14	1.4	0.41	0.30	2.7	6.3	6.3

Table 1. Maximum velocity defect, mean velocity half-width and spatial resolution of the probe at the wake centreline of three x/d positions.

Table 1 gives the maximum velocity defect, mean velocity half-width and spatial resolution of the probe in terms of the Kolmogorov length scale at the wake centerline of the local x/d position. The value of $\overline{\varepsilon}$ is estimated using local homogeneity in the transverse plane (equation (5)) which, according to Lefeuvre *et al.* [8] as well as our own results (see next section), should be more accurate in the intermediate wake than if local isotropy is assumed. The detailed description of the experimental set-up and estimation of the experimental uncertainty is available in [13] and will not be repeated here.

Results and Discussion

Before further investigation, the spatial resolution of the probe is examined. The present $\overline{(\partial u/\partial y)^2}$ at x/d=10 and 40 is compared in Figure 2 with the measurement by Mi and Antonia [9]. They examined the local axisymmetry assumption for x/d = 10-70 (Re = 3000) using two x-wires with a better spatial resolution of about 8η at x/d = 10 and 5η at x/d = 40, which are quite close to the optimum spatial resolution of about 4η [13]. The agreement between the two sets of data is quite well, especially at x/d = 40. The attenuation of the present probe appears only evident at the range close to the wake centreline at x/d = 10 (y/L<0.3). A more detailed data validation, including the variances of velocity and vorticity fluctuations has already been made in [13].

Because of the difficulty in measuring all the twelve components in $\overline{\varepsilon}$ (equation (1)), the expression of $\overline{\varepsilon}$ is often simplified based on different assumptions. The most widely employed estimate assumes local isotropy, i.e.

$$\overline{\varepsilon_{iso}} = 15\nu\overline{(u_{1,1})^2} \qquad (2)$$

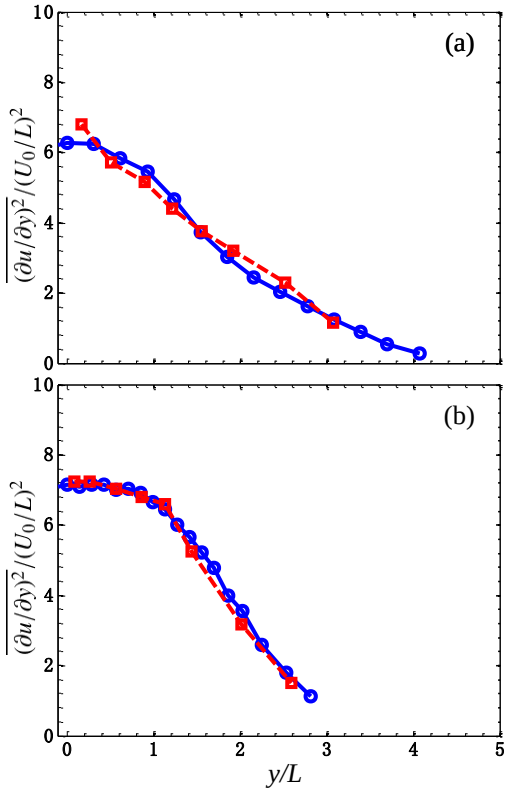

Figure 2. Comparison of $\overline{(\partial u/\partial y)^2}$ between the present data (blue circles with solid line) and those from Mi and Antonia [9] (red squares with dash line): (a) x/d=10, (b) 40.

Another estimate is based on local homogeneity, i.e.

$$\overline{\varepsilon}_{hom} = \nu\overline{\omega^2} \qquad (3)$$

where $\overline{\omega^2} \equiv \overline{(\omega_1^2 + \omega_2^2 + \omega_3^3)}$ is the mean enstrophy, and ω_i is the vorticity fluctuation in the i direction. Antonia *et al.* [1] found that this equality is satisfied approximately across a fully developed channel flow. The expression based on the assumption of local axisymmetry, first suggested by George and Hussein [4], is given by

$$\overline{\varepsilon}_a = \nu\left(\frac{5}{3}\overline{u_{1,1}^2} + 2\overline{u_{1,3}^2} + 2\overline{u_{2,1}^2} + \frac{8}{3}\overline{u_{2,3}^2}\right). \qquad (4)$$

Zhu and Antonia [15] proposed another expression for estimating the energy dissipation rate by assuming local homogeneity in the transverse (y, z) plane in a cylinder wake, viz.

$$\begin{aligned}\overline{\varepsilon}_{yz} =& \nu\Big(4\overline{(u_{1,1})^2} + \overline{(u_{1,2})^2} + \overline{(u_{1,3})^2} \\ &+ \overline{(u_{2,1})^2} + \overline{(u_{2,3})^2} + \overline{(u_{3,1})^2} + \overline{(u_{3,2})^2} \\ &+ 2\overline{(u_{1,2}u_{2,1})} + 2\overline{(u_{1,3}u_{3,1})} - 2\overline{(u_{2,3}u_{3,2})}\Big)\end{aligned} \qquad (5)$$

All the terms involved in equations (2) - (5) are now measured directly by the present probe, thus allowing an examination of these different surrogates of the energy dissipation rate.

Djenidi and Antonia [3] proposed a spectral chart method for estimating the true value of the energy dissipation rate based on the universality of the velocity spectrum, normalized by Kolmogorov scales, in the dissipative range. The basic idea of the method is to first 'guess' values of the energy dissipation rate in order to 'un-normalize' a reference universal spectrum iteratively until it collapses onto the measured velocity spectrum. In the

present study, the reference 'true' value of the energy dissipation rate is estimated by applying this spectral chart method to the measured streamwise velocity fluctuation.

Figure 3 presents the results of equations (2) - (5) and the true value estimated via the spectral chart method in [3] at the wake centreline of the three *x/d* positions. While $\overline{\varepsilon}_{iso}$ overestimates the true value by about 32% ~ 18% at *x/d* = 10 and 20. $\overline{\varepsilon}_{hom}$ and $\overline{\varepsilon}_{a}$ may underestimate the true value by about 41% ~ 29% and 57% ~ 45%, respectively. $\overline{\varepsilon}_{yz}$ provides the most accurate estimation within the errors of about 10% and 5% at *x/d* = 10 and 20, respectively. At *x/d* = 40, the departures between different surrogates shrink and the estimations agree well with each other. It may be concluded that $\overline{\varepsilon}_{yz}$ is the most accurate estimation of the turbulent energy dissipation rate, especially at smaller *x/d*. This is fully consistent with the observation in the intermediate wake of a square cylinder based on DNS data [8]. This is not unexpected since $\overline{\varepsilon}_{yz}$ contains virtually all the terms that make up the true energy dissipation in equation (1).

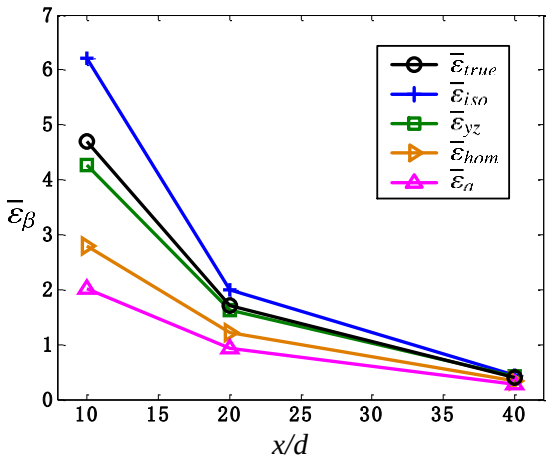

Figure 3. Comparison between different surrogates of $\overline{\varepsilon}$ on the centreline at *x/d* = 10, 20 and 40.

A very distinct feature in the intermediate wake is the dominance Kármán vortex street at small *x/d*, followed by its gradual weakening and eventual disappearance as *x/d* increases. Therefore, it is of great importance and interest to investigate the spatial distribution of the turbulent energy dissipation rate in the context of this feature. As indicated by figure 3, the estimation $\overline{\varepsilon}_{yz}$ provides quite a good approximation to the true value of the energy dissipation rate. Naturally the spatial distribution of the energy dissipation rate is not surprisingly reflected by that of $\overline{\varepsilon}_{yz}$. In order to examine the spatial structure of the energy dissipation rate, a phase averaged technique is employed to separate the coherent scale from the remaining smaller scales of ε_{yz}.

The phase average of an instantaneous quantity Γ is given by $\langle\Gamma\rangle = 1/N \sum_{i=1}^{N} \Gamma_{k,i}$ where k represents phase. N is the total number of detections, about 1800, 1700 and 400 at *x/d*=10, 20 and 40, respectively. Based on the triple decomposition [5], Γ can be viewed as the sum of the time mean component $\overline{\Gamma}$ and the fluctuating component β. The latter can be further decomposed into a coherent fluctuation $\widetilde{\beta}$ and a remainder $\langle\beta\rangle_r$, viz. $\beta = \widetilde{\beta} + \langle\beta\rangle_r$. The $\widetilde{\beta} \equiv \langle\beta\rangle$ originates from the large-scale coherent structures, while $\langle\beta\rangle_r$ is referred to as the remainder fluctuation.

Figure 4 shows the phase-averaged coherent energy dissipation rate $\widetilde{\varepsilon}_{yz}$ and the remainder $\langle\varepsilon_{yz}\rangle_r$ at *x/d* =10, 20 and 40. The phase ϕ, ranging from -2π to 2π, can be interpreted as a longitudinal distance based on Taylor's hypothesis, $\phi = 0 \sim 2\pi$ corresponding to the averaged vortex wavelength. To avoid any distortion of the physical space, the same scales are used in the ϕ and *y/d* directions. The positions of the centres and saddle points [14], identified from the phase-averaged sectional streamlines (not shown), are marked by '+' and '×', respectively. The thicker broken line denotes the outermost vorticity contours of $\widetilde{\omega}_z$ (not shown), which is about 25% of the maximum magnitude $|\widetilde{\omega}_z|$. This contour provides a reference for the periphery of the Kármán vortex. The dash dotted line passing through the saddle point represents the diverging separatrix. Flow is from left to right.

It can be seen that the coherent (figure 4(a)-(c)) and remaining (figure 4(d)-(f)) components are quite different at all three *x/d* positions. It is not surprising that the remaining small scales essentially contribute most to the energy dissipation rate. The coherent component $\widetilde{\varepsilon}_{yz}$ concentrates on the front and back of the vortex, which is mostly from the contribution of $\widetilde{u_{1,2}}^2$ term (not shown). The remaining small scales component mainly distribute within the Karman vortex, with the maxima near the vortex centre. Note that at *x/d*=40, the concentrations of both $\widetilde{\varepsilon}_{yz}$ (figure 4(c)) and $\langle\varepsilon_{yz}\rangle_r$ (figure 4(f)) are smeared mostly as the vortices are quite weak and in the process of breaking up [13]. The observation is consistent with Hussain and Hayakawa's [6] finding that the incoherent turbulence intensity occurs largely within the Kármán vortex at *x/d*=10-40 and its peaks almost coincide with the vortex centre. Since the turbulent energy dissipation rate physically reflects the rate of the turbulent energy transforming into heat at small scales, its spatial distribution is expected to be associated with that of the incoherent or small-scale turbulent energy.

Hussain and Hayakawa [6] proposed a topological model for explaining the mechanism of the turbulent plane wake. However, since the energy dissipation rate was not measured, the model did not provide any information on the distribution of the energy dissipation. Figure 4 show unequivocally that the turbulent energy dissipation is concentrated within the spanwise vortex. As a result, a more complete picture for the turbulence dynamics may be cast presently by incorporating the information on the energy dissipation into Hussain and Hayakawa's [6] model, as shown in figure 5. In the new model, the saddle region (denoted as A), where intense strain is induced by the rotating motion of successive vortices, can be identified with the turbulent energy production area. The non-turbulent fluid from the free stream is engulfed into the rotational motion of the ribs (or quasi-streamwise vortex) and is subjected to the vortex stretching by the strain along the diverging separatrix, leading to the production of turbulence. Turbulent mixing will mostly occur at the region (denoted as B_1 & B_2) where the streamwise vortex and the spanwise vortex are in contact with each other since the direct interaction between the two near orthogonal vortex structures can produce three-dimensional vorticity fluctuations. The turbulence, thus produced, will then be entrained by the rotational motion of the spanwise vortex and accumulated within the vortex structure before being finally dissipated.

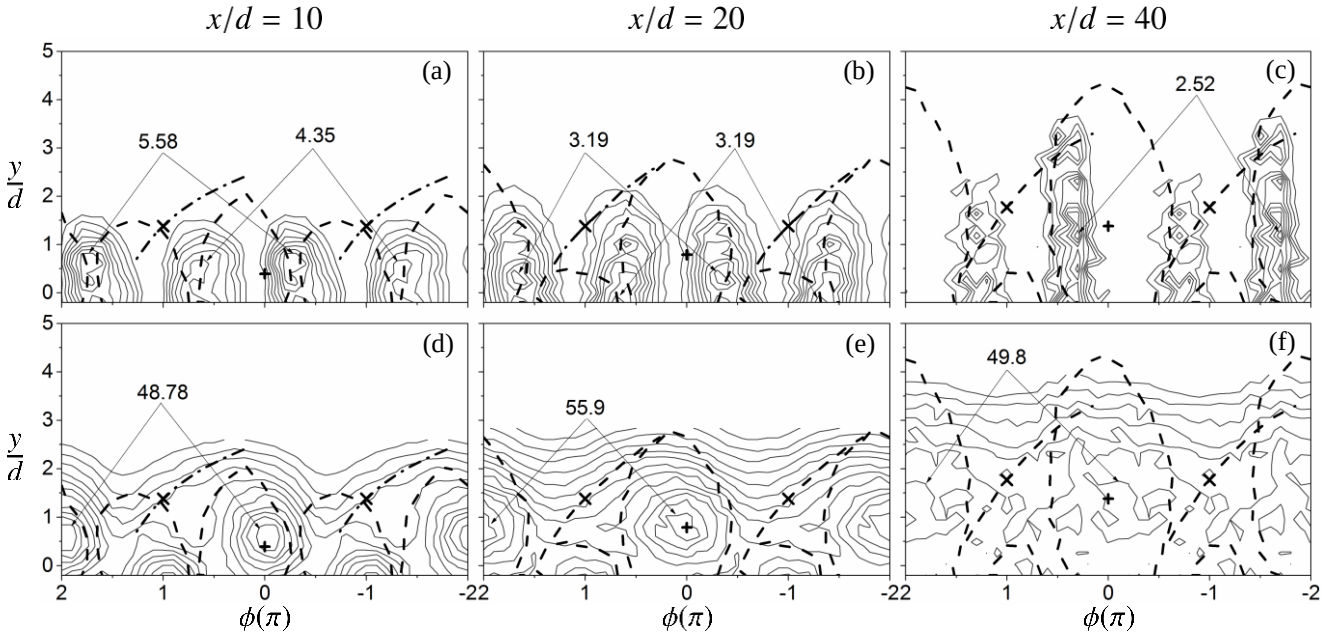

Figure 4. Phase averaged coherent turbulent energy dissipation rate $\widetilde{\varepsilon}_{yz}/(U_0/L)^2$ ((a)-(c)) and the remainder $\langle\varepsilon_{yz}\rangle_r/(U_0/L)^2$ ((d)-(f)) at all three *x/d* positions. Contour levels: (a)-(c): 0.62, 0.35, 0.28; (d)-(f): 4.4, 3.9, 6.0.

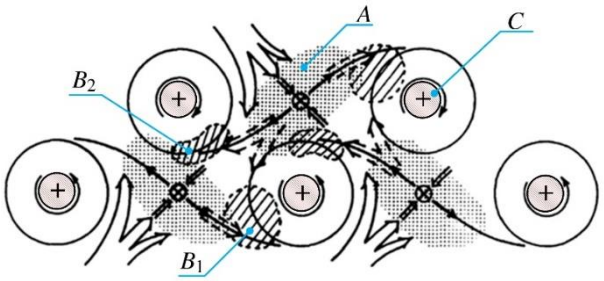

Figure 5. Topological model of flow in a plane wake. **+,** vortex centre; ×, saddle point; ⟹ engulfed non-turbulent fluid; ⇢⇢ flow of produced turbulence; A: turbulence production; B_1 & B_2: turbulent mixing; C: turbulent kinetic energy dissipation.

Conclusions

The estimation of the turbulent energy dissipation rate $\bar{\varepsilon}_{yz}$ based on the assumption of local homogeneity in the transverse plane provides the most accurate surrogate of the true value of $\bar{\varepsilon}$. The energy dissipation rate is concentrated mainly within the spanwise vortex rollers rather than in regions where strong turbulent mixing takes place. A more complete topological picture, which incorporates the new information for the energy dissipation into Hussain and Hayakawa's [6] model, is proposed (Fig 5).

Acknowledgments

YZ is grateful for the financial support from NSFC through grant 51421063 and from Scientific Research Fund of Shenzhen Government through grant KQCX2014052114430139.

References

[1] Antonia, R.A., Kim, J. & Browne, L., Some characteristics of small-scale turbulence in a turbulent duct flow, *J. Fluid Mech.*, **233**, 1991, 369-388.

[2] Browne, L., Antonia, R.A. & Shah, D.A., Turbulent energy dissipation in a wake, *J. Fluid Mech.*, **179**, 1987, 307-326.

[3] Djenidi, L. & Antonia, R.A., A spectral chart method for estimating the mean turbulent kinetic energy dissipation rate, *Exp. Fluids*., **53**, 2012, 1005-1013.

[4] George, W. & Hussein, H., Locally axisymmetric turbulence, *J. Fluid* Mech., **233**, 1991, 1-23.

[5] Hussain, A., Coherent structures—reality and myth, *Phys. Fluids*., **26**, 1983, 2816-2850.

[6] Hussain, A. & Hayakawa, M., Eduction of large-scale organized structures in a turbulent plane wake, *J. Fluid Mech*., **180**, 1987, 193-229.

[7] Landau, L.D. & Lifshitz, E.M., Fluid mechanics, 1959,

[8] Lefeuvre, N., Thiesset, F., Djenidi, L. & Antonia, R.A., Statistics of the turbulent kinetic energy dissipation rate and its surrogates in a square cylinder wake flow, *Phys. Fluids*., **26**, 2014, 095104.

[9] Mi, J. & Antonia, R.A., Approach to local axisymmetry in a turbulent cylinder wake, *Exp. Fluids*., 48, 2010, 933-947.

[10] Sreenivasan, K.R. & Antonia, R.A., The phenomenology of small-scale turbulence, *Annu. Rev. Fluid Mech.*, **29**, 1997, 435-472.

[11] Tang, S.L., Antonia, R.A., Djenidi, L. & Zhou, Y., Transport equation for the isotropic turbulent energy dissipation rate in the far-wake of a circular cylinder, *J. Fluid Mech.*, **784**, 2015, 109-129.

[12] Thiesset, F., Danaila, L. & Antonia, R.A., Dynamical effect of the total strain induced by the coherent motion on local isotropy in a wake, *J. Fluid Mech.*, **720**, 2013, 393-423.

[13] Zhou, T., Zhou, Y., Yiu, M.W. & Chua, L.P., Three-dimensional vorticity in a turbulent cylinder wake, *Exp. Fluids*., **35**, 2003, 459-471.

[14] Zhou, Y. & Antonia, R.A., Critical points in a turbulent near wake, *J. Fluid* Mech., **275**, 1994, 59-82.

[15] Zhu, Y. & Antonia, R.A., On the correlation between enstrophy and energy dissipation rate in a turbulent wake, *Appl. Sci. Res.*, **57**, 1997, 337-347.